Classifying Enzymes from Selectivity Fingerprints

Johann Grognux and Jean-Louis Reymond*[a]

Fingerprints of lipases and esterases have been recorded by using an array of chiral fluorogenic aliphatic esters of increasing chain length (C_4–C_{16}). Classification of the enzyme series was carried out with selectivity data by clustering and principal component analysis (PCA). Enzymes were classified on the basis of selectivity for chain length (C_4–C_6 vs. C_{10}–C_{16}) and of middle-chain-length (C_8–C_{10}) reactivity. A minimum set of nine substrates was defined by cluster analysis of relative reactivities of each substrate for the different enzymes. This selectivity-based analysis is general. It does not require a common reference substrate to react with all enzymes or vice versa, and is independent of knowing the exact concentration of active protein in the enzyme samples.

Introduction

Thousands of different enzymes have been discovered through the exploration of biodiversity and by mutation studies.[1] Enzymes may be classified according to their source organism, their genetic sequence, their three-dimensional structural type, and their functionality. Chemical functional information, such as chemo- and stereoselectivities within given reaction types, is particularly relevant to the practical application of enzymes. In contrast to sequence data, catalysis data spanning large numbers of different substrates and enzymes are extremely rare.[2] Furthermore, no general method has been described for extracting functional classification from such data. Herein we report a method for functional analysis and classification of enzymes using the example of lipases and esterases with data from an array of fluorogenic substrates. The substrate array consists of a chain-length series of aliphatic esters of a common fluorogenic glycerol-type chiral alcohol. This array is tailored to distinguish between esterase-like (short-chain aliphatic acid) and lipase-like (long-chain aliphatic acid) reactivities.

Results and Discussion

Enzyme assays are protocols that detect the activity of certain enzymes.[3] Most enzyme assays include only one or two test substrates under well-defined conditions, and interesting chemical parameters such as chemo- and stereoselectivity profiles are not accessible. We recently reported that assaying hydrolytic enzymes with arrays of periodate-activated chromogenic and fluorogenic substrates provides rapid access to chemo- and stereoselectivity fingerprints.[4] Long-chain aliphatic esters of diol **9** were subsequently found to be particularly sensitive and selective substrates for lipases and esterases.[5] We set out to develop a general analysis protocol for enzyme fingerprints at the example of these sensitive and selective lipase/esterase probes.

An array of (*R*)- and (*S*)-configured monoesters, **1**–**8**, of diol **9** with aliphatic esters of varying chain length was prepared by selective monoesterification with the acyl chloride and collidine or triethylamine as base. The acetate ester was not used because its reactivity with the different enzymes had been found earlier to be much weaker than that of butyrate and longer-chain esters. The substrate array thus obtained was used for fingerprint analysis of 25 different lipases and esterases (Scheme 1). After ester hydrolysis by the enzyme, umbellifer-

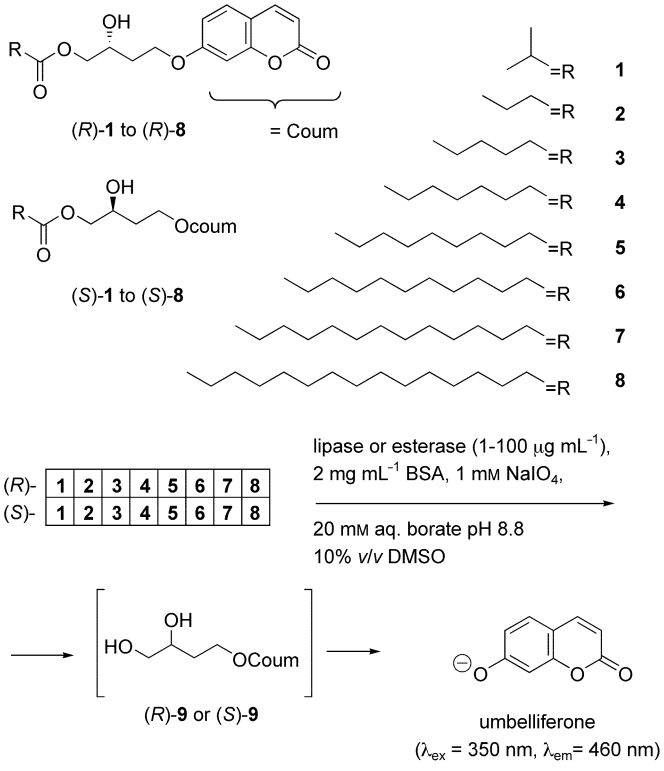

Scheme 1. *Fingerprint measurement with fluorogenic substrate array.*

[a] *J. Grognux, Prof. Dr. J.-L. Reymond*
Department of Chemistry and Biochemistry, University of Bern
Freiestrasse 3, 3012 Bern (Switzerland)
Fax: (+41) 316-318-057

  DOI: 10.1002/cbic.200300779

one is rapidly released from the primary hydrolysis product **9** by oxidative diol cleavage with $NaIO_4$ and subsequent β-elimination under catalysis with bovine serum albumin (BSA). The advantage of this indirect release strategy lies in the chemical stability of the enzyme-reactive ester bond in substrates **1**–**8**, which is such that background hydrolysis is negligible. All assays (16 per enzyme, 0.1 mL each) were carried out in 96-well microtiter plates by monitoring the formation of the fluorescent product umbelliferone with a fluorescence microtiterplate reader. The best reproducibility in reaction rates was obtained with 10% *v/v* dimethylsulfoxide as cosolvent, in particular with the C_{12} to C_{16} esters, which otherwise showed sluggish reactivity. Enzyme were measured at dilutions of 1, 10, and 100 $\mu g\,mL^{-1}$, and the lowest enzyme concentration to give good catalysis signals was used for data processing. The resulting fingerprints are summarized in Figure 1 as two-color coded eight-position bars, with each position showing the combined data of an enantiomeric pair with the color intensity proportional to activity and the green–purple balance coding enantioselectivity.[6]

Analyzing reaction-rate data in principle requires knowledge of the concentration of active enzyme in the sample, which varies enormously depending on purification and intrinsic enzyme stability. A functional classification should not be exposed to biases and errors from such parameters. Activity units (U, $\mu mol\,min^{-1}$ per mg protein) could not be used for normalization because reference substrates and reaction conditions to measure these units also vary between different enzymes. To circumvent that problem, the rate data were analyzed in terms of selectivity only. For each enzyme, the relative reactivity of each substrate was reported as a percentage of the total reactivity observed with this enzyme across all substrates. This selectivity analysis eliminated the need for a reference substrate that would react with all enzymes tested.

The dataset was processed by using the multivariate analysis software packages *Winidams* and *Vista*.[7] The sixteen substrates

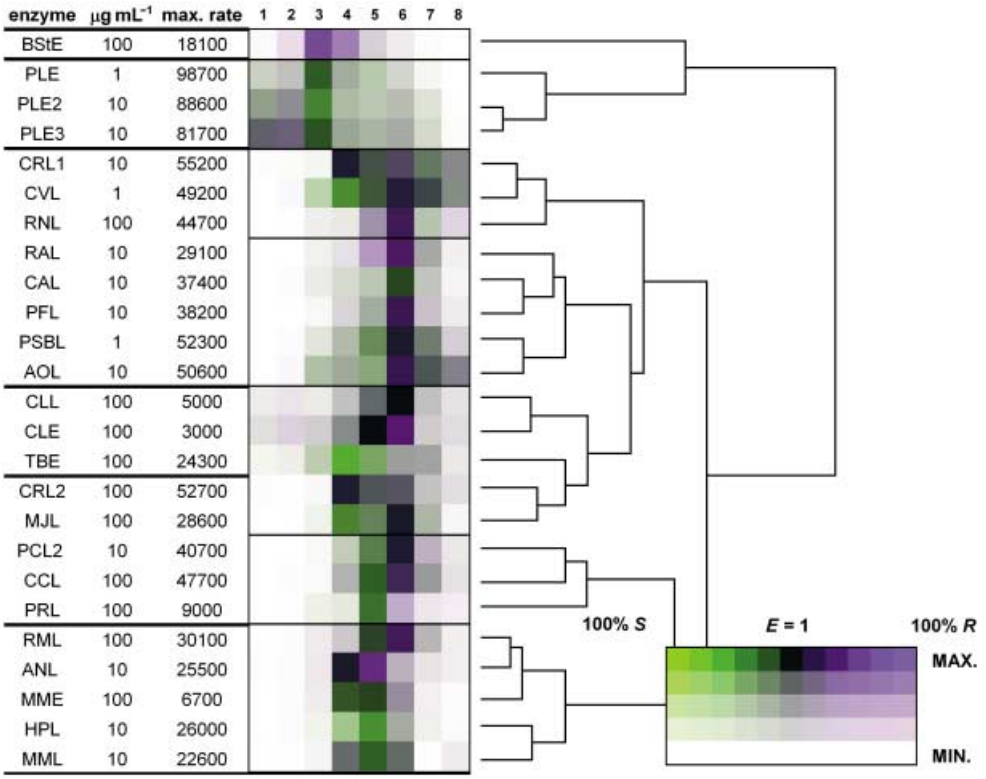

Figure 1. *Lipase/esterase fingerprints and hierarchical tree. Each line represents a different enzyme, and each column represents a different substrate. Each colored square represents the reaction rates of two enantiomeric lipase substrates (measured separately) relative to the maximum rate observed with the corresponding enzyme (line), which is given in* $pm\,s^{-1}$ *(color key at lower right). The two-color display was generated from the rate data as described before.*[4c] *Hierarchical agglomerative clustering was carried out by using Ward's method on the basis of standardized euclidean distances.*[7b,8] *0.1 mL assays were carried out in 96-well round-bottom polypropylene microtiter plates (Costar) under the following conditions: 20 mM aq. borate buffer, pH 8.8, 10% v/v DMSO, 100 μM substrate, 1–100* $\mu g\,mL^{-1}$ *enzyme, 1 mM* $NaIO_4$*, 2 mg.mL*$^{-1}$ *BSA, 30°C, 2 h. The fluorescence increase was recorded with a Cytofluor II fluorescence plate reader (Perseptive Biosystems, filters* $\lambda_{ex} = 360 \pm 20$*,* $\lambda_{em} = 460 \pm 20$ *nm) and converted to umbelliferone concentration by using a calibration curve. The steepest linear portion of each curve was used to calculate the reaction rate in each assay. Enzymes are from Fluka or Roche: BStE* Bacillus stearothermophilus *esterase F46051; PLE pig liver esterase F46058; PLE2 pig liver esterase fraction 1 Roche Chirazyme; PLE3 pig liver esterase fraction 2 Roche Chirazyme; CRL1* Candida rugosa *lipase purified Roche Chirazyme L3P; CVL:* Chromobacterium viscosum *lipoprotein lipase F62333; RNL* Rhizopus niveus *lipase F62310; RAL* Rhizopus arrhizus *lipase F62305; CAL* Candida antarctica *lipase F62299; PFL* Pseudomonas fluorescens *lipase F62321; PSBL* Pseudomonas sp. *Type B lipoprotein lipase F62336; AOL* Aspergillus oryzae *lipase F62285; CLL* Candida lipolytica *lipase F62303; CLE* Candida lipolytica *esterase F46056; TBE* Thermoanaerobium brockii *esterase F46061; CRL2* Candida rugosa *lipase Roche Chirazyme L3; MJL* Mucor javanicus *lipase F62304; PCL2* Pseudomonas cepacia *lipase F62309; CCL Candida cylindracea lipase F62316; PRL* Penicillium roqueforti *lipase F62308; RML* Rhizomucor miehei *lipase F62291; ANL* Aspergillus niger *lipase F62294; MME* Mucor miehei *esterase F46059; HPL hog pancreatic lipase F62300; MML* Mucor miehei *lipase F62298.*

were defined as variables and the twenty-five enzymes tested as observations. Cluster analysis is based on algorithms that group observations on the basis of their spatial proximity in an *N*-dimensional space defined by *N* variables.[8] Clustering was carried out by using Ward's method on the basis of standardized euclidean distances. The dataset in its clustered form was represented as the hierarchical tree (Figure 1). The clustered data corresponded well with six visually identifiable groups of enzymes A–F in the two-dimensional projection of observations (enzymes) along the first two principal components (PC) (Figure 2). Analysis of PC coefficients per substrate

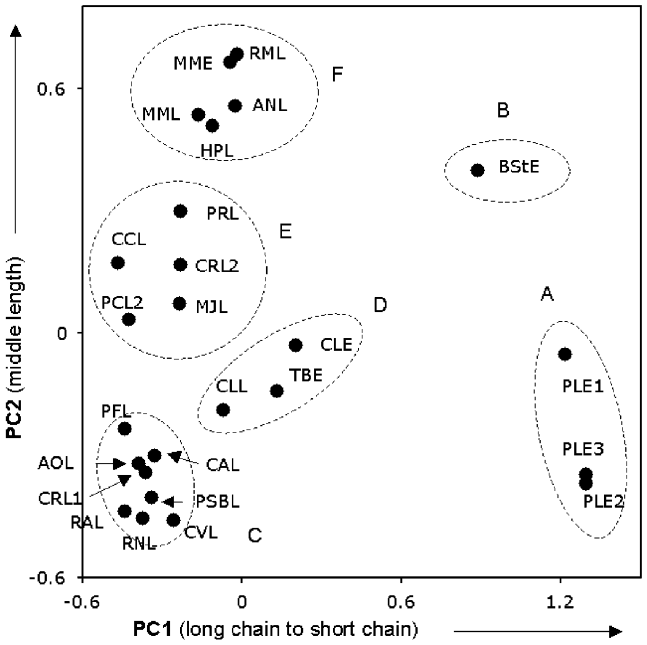

Figure 2. *Projection of enzymes according to principal components PC1 and PC2. The groups A–F identified visually (dashed ellipses) correspond to those obtained by agglomerative clustering, with the exception of CRL2 and MJL in cluster E, which are assigned to cluster D (see Figure 1).*

(Figure 3) showed that PC1 reflected the short-chain (C_4–C_6) versus long-chain (C_{10}–C_{16}) reactivity, and PC2 a selective enhancement of middle chain (C_8–C_{10}) reactivity. Groups A and B, which contained four esterases and two esterases from group D, were present at positive PC1 values; this is in agreement with the usually stronger reactivity of esterases with short-chain aliphatic esters. The other four groups were situated at smaller or negative PC1 values; this indicates a preference for longer-chain esters.

We next addressed the question of defining the minimal set of substrates necessary for generating the observed clusters. All substrates had significant coefficients in the main principal components; this excluded the a priori elimination of any of them (Figure 3). Functional equivalence between substrates was analyzed by clustering the dataset with enzymes as variables and substrates as observations. In this perspective, any two substrates showing comparable reactivity profiles across the different enzymes would appear as very similar, and therefore functionally equivalent; this would mean that only one of

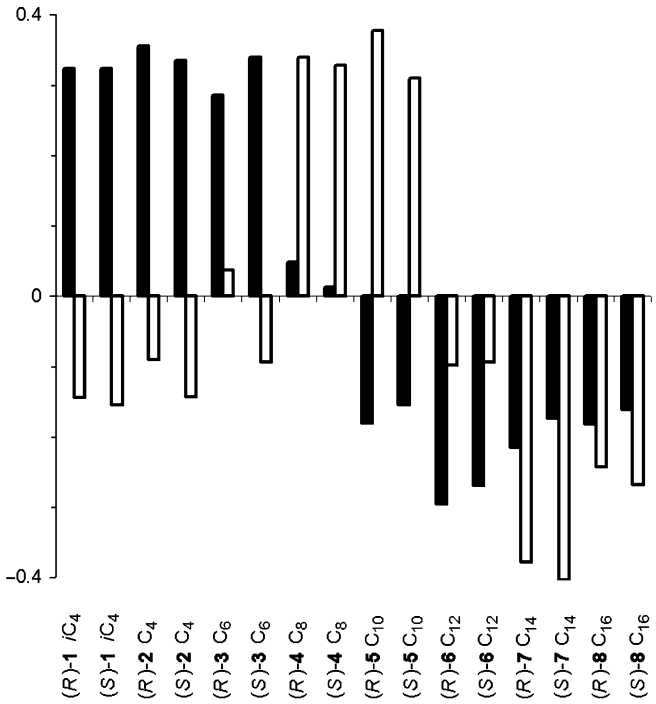

Figure 3. *Coefficients per substrate of the first two principal components (PC), which account for 68% of observed variability : PC1 = 46% (black bars), PC2 = 22% (white bars).*

these two substrates should be sufficient to produce the observed enzyme-classification data. The substrate dataset was clustered by agglomerative clustering.[7a,8] While clustered data are often represented as hierarchical trees (as in Figure 1), a gray-scale representation of the distance matrix was selected to visualize similarities in this case, since clustering did not produce a significant reordering of the substrate series (Figure 4). The distance matrix represents the euclidean distance between

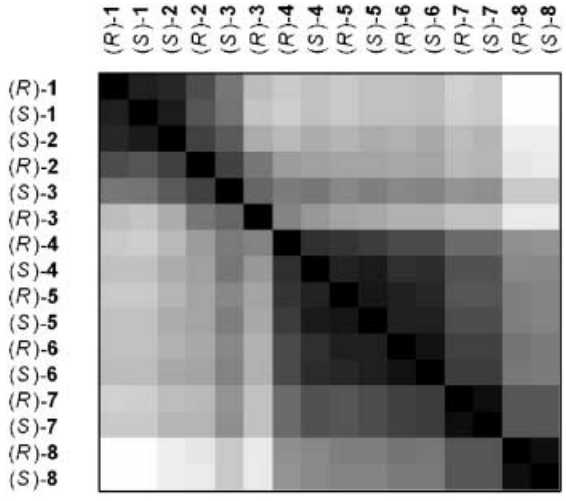

Figure 4. *Euclidean distance matrix between substrates **1**–**8** in the 25-dimensional space of enzyme reaction rate, rendered in grayscale (black: distance = 0, white: maximum distance). For each substrate, reactivity for each enzyme was expressed as percent of the total reactivity observed with this substrate across all enzymes measured. Substrates were clustered by agglomerative clustering by using the group-average method.*[7a,8]

substrates in the 25-dimensional space of enzyme reaction rates and the gray-scale representation reveals clusters as larger dark squares along the diagonal. The minimal cluster size is a single substrate, which is shown in black along the diagonal for identity. Analysis of this distance matrix revealed that substrates were clustered into five groups: the C_4 esters (*S*)-**2**, (*R*)-**1** and (*S*)-**1**, the C_8 ester (*R*)-**4** with the C_{10} esters (*R*)-**5** and (*S*)-**5**, and each of the C_{12}, C_{14}, and C_{16} enantiomeric pairs **6**, **7**, and **8**. Butyrate (*R*)-**2**, octanoate (*R*)-**4**, and hexanoates (*R*)-**3** and (*S*)-**3** remained as individuals. This analysis suggested that a selection of nine out of sixteen substrates should give the same clustering of enzymes as that obtained with all sixteen substrates. Indeed a reduced set consisting of (*S*)-**1**, (*R*)-**2**, (*S*)-**3**, (*R*)-**3**, (*R*)-**4**, (*S*)-**5**, (*S*)-**6**, (*S*)-**7** and (*S*)-**8** clustered the enzymes almost identically. Further reduction of the number of substrates destroyed the cluster structure.

Conclusion

In summary, selectivity fingerprints of twenty-five lipases and esterases were recorded with an array of sixteen chiral fluorogenic substrates and analyzed by clustering and principal-component analysis; this led to the definition of enzyme subgroups. Analyzing selectivities rather than reaction rates led to a classification that was independent of activity units of a reference substrate common to all enzymes, and without knowledge of the exact enzyme concentration in each sample studied. The long-chain (C_{10}–C_{16}) versus short-chain (C_4–C_6) ester-reactivity balance (PC1) and the selective enhancement of middle-chain (C_8–C_{10}) reactivity (PC2) appeared as key clustering determinants. These parameters represent refined versions of the standard C_4 versus C_8 ester reactivity used to distinguish lipases from esterases. Clustering substrates against enzymes revealed functional equivalences and a minimal set of nine substrates sufficient for enzyme classification. The analysis can be propagated by including more enzymes and re-expanding the minimal substrate set to include further structural types. The method can also be extended to other types of enzymes and catalysts. This might eventually lead to a canonical substrate array suitable for a broad classification of already known and newly discovered enzymes on the basis of their selectivity fingerprints.

Experimental Section

General: All reactions were followed by TLC on Alugram SIL G/UV_{254} silica gel sheets (Macherey–Nagel) with detection by UV light or with 0.5% phosphomolybdic acid solution in 95% EtOH. Silica gel 60 (Macherey–Nagel 230–400 mesh) was used for flash chromatography (FC). Melting points were determined on a Kofler apparatus or with a Büchi 510 apparatus and are uncorrected. ^{1}H and ^{13}C NMR spectra were recorded with a Bruker AC-300 or a BRUKER DMX 400 spectrometer.

(*S*)-7-(3-hydroxy-4-*iso*butyroxybutyloxy)-2*H*-1-benzopyran-2-one ((*S*)-1)

Typical synthetic procedure: Triethylamine (83.5 μL, 0.60 mmol, 2.0 equiv) was added to the diol (*S*)-**9** (75.0 mg, 0.60 mmol, 1.0 equiv) previously dissolved in dry dichloromethane (3.4 mL), and the mixture was cooled to −5 °C. Isobutyryl chloride (31.5 μL, 0.30 mmol, 1.0 equiv) was added dropwise. The solution was stirred at −5 °C for 30 min and then at RT for 4.5 h. The solution was then washed with H_3PO_4 (0.25 M), and the organic layer was dried over $MgSO_4$ and concentrated in vacuo. The resulting crude mixture was purified by flash chromatography (EtOAc/hexane 1:1) yielding 49 mg (51%) of a colorless oil. $[\alpha]_D^{20} = -6.6$ ($c = 0.6$ in $CHCl_3$); ^{1}H NMR (300 MHz, $CDCl_3$): $\delta = 7.64$ (d, $J = 9.6$ Hz, 1H), 7.38 (dd, $J = 7.4$, 1.8 Hz, 1H), 6.87–6.84 (m, 2H), 6.27 (d, $J = 9.5$ Hz, 1H), 4.30–4.06 (m, 5H), 2.63 (septet, $J = 7.0$ Hz, 1H), 2.09–1.90 (m, 2H), 1.21 (d, $J = 7.0$ Hz, 6H); ^{13}C NMR (75 MHz, $CDCl_3$): $\delta = 174.15$, 162.03, 161.33, 156.02, 143.51, 128.94, 113.40, 112.96 (2C), 101.66, 68.54, 67.45, 65.15, 34.11, 32.74, 19.16 (2C); HRMS(ESI-MS): calcd for ($C_{17}H_{21}O_6$) $[M+H]^+$: 321.1338, found: 321.1346.

(*R*)-7-(3-hydroxy-4-*iso*-butyroxybutyloxy)-2*H*-1-benzopyran-2-one ((*R*)-1): Application of the typical procedure with diol (*R*)-**9** (115 mg, 0.46 mmol, 1.0 equiv), collidine (122 μL, 0.92 mmol, 2.0 equiv), and isobutyroyl chloride (78.0 μL, 0.74 mmol, 1.6 equiv) gave (*R*)-**1** (105 mg, 71.2%) as a colorless oil; $[\alpha]_D^{20} = +6.8$ ($c = 0.55$ in $CHCl_3$); HRMS(EI-MS): calcd for ($C_{17}H_{20}O_6$) $[M]^+$: 320.1260, found: 320.1259.

(*S*)-7-(3-hydroxy-4-butyroxybutyloxy)-2*H*-1-benzopyran-2-one ((*S*)-2): Application of the typical procedure with diol (*S*)-**9** (78 mg, 0.31 mmol, 1.0 equiv), collidine (83 μL, 0.62 mmol, 2.0 equiv), and butyroyl chloride (49 μL, 0.47 mmol, 1.5 equiv) gave (*S*)-**2** (105 mg, 71.2%) as a colorless oil; $[\alpha]_D^{20} = -6.0$ ($c = 0.50$ in $CHCl_3$); ^{1}H NMR (300 MHz, $CDCl_3$): $\delta = 7.64$ (d, $J = 9.6$ Hz, 1H), 7.40–7.37 (m, 1H), 6.87–6.84 (m, 2H), 6.27 (d, $J = 9.5$ Hz, 1H), 4.30–4.05 (m, 5H), 2.36 (t, $J = 7.4$ Hz, 1H), 2.10–1.90 (m, 2H), 1.69 (sextet, $J = 7.4$ Hz, 2H), 0.98 (t, $J = 7.4$ Hz, 3H); ^{13}C NMR (100 MHz, $CDCl_3$): $\delta = 173.91$, 162.04, 161.33, 155.85, 143.54, 128.87, 113.12, 112.91, 112.68, 101.54, 68.36, 67.04, 65.09, 36.10, 32.76, 18.47, 13.71; HRMS(EI-MS): calcd for ($C_{17}H_{20}O_6$) $[M]^+$: 320.1260, found: 320.1260.

(*R*)-7-(3-hydroxy-4-butyroxybutyloxy)-2*H*-1-benzopyran-2-one ((*R*)-2): Application of the typical procedure with diol (*R*)-**9** (90 mg, 0.36 mmol, 1.0 equiv), collidine (95 μL, 0.72 mmol, 2.0 equiv), and butyroyl chloride (38 μL, 0.47 mmol, 1.3 equiv) gave (*R*)-**2** (89 mg, 77%) as a colorless oil; $[\alpha]_D^{20} = +5.7$ ($c = 0.50$ in $CHCl_3$); HRMS(EI-MS): calcd for ($C_{17}H_{20}O_6$) $[M]^+$: 320.1260, found: 320.1261.

(*S*)-7-(3-hydroxy-4-hexanoyloxybutyloxy)-2*H*-1-benzopyran-2-one ((*S*)-3): Application of the typical procedure with diol (*S*)-**9** (75 mg, 0.30 mmol, 1.0 equiv), triethylamine (84 μL, 0.60 mmol), and hexanoyl chloride (46 μL, 0.33 mmol, 1.1 equiv) gave (*S*)-**3** (80 mg, 76%) as a colorless oil; $[\alpha]_D^{20} = -5.1$ ($c = 0.35$ in $CHCl_3$); ^{1}H NMR (400 MHz, $CDCl_3$): $\delta = 7.64$ (d, $J = 9.5$ Hz, 1H), 7.37 (m, 1H), 6.86–6.83 (m, 2H), 6.26 (d, $J = 9.5$ Hz, 1H), 4.28–4.06 (m, 5H), 2.36 (t, $J = 7.6$ Hz, 2H), 2.08–1.91 (m, 2H), 1.69–1.58 (m, 2H), 1.33–1.23 (m, 4H), 0.90 (m, 3H); ^{13}C NMR (75 MHz, $CDCl_3$): $\delta = 174.17$, 162.04, 161.35, 155.98, 143.53, 128.93, 113.37, 113.33, 112.96, 101.63, 68.48, 67.31, 65.14, 34.26, 32.75, 31.41, 24.74, 22.42, 14.03; HRMS(EI-MS): calcd for ($C_{19}H_{25}O_6$) $[M+H]^+$: 348.1572, found: 348.1572.

(*R*)-7-(3-hydroxy-4-hexanoyloxybutyloxy)-2*H*-1-benzopyran-2-one ((*R*)-3): Application of the typical procedure with diol (*R*)-**9** (90 mg, 0.36 mmol, 1.0 equiv), collidine (95 μL, 0.72 mmol), and hexanoyl chloride (65 μL, 0.47 mmol, 1.3 equiv) gave (*R*)-**3** (80 mg, 76%) as a colorless oil; $[\alpha]_D^{20} = +5.2$ ($c = 0.40$ in $CHCl_3$); HRMS(EI-MS): calcd for ($C_{19}H_{24}O_6$) $[M]^+$: 348.1573, found: 348.1572.

(*S*)-7-(3-hydroxy-4-octanoyloxybutyloxy)-2*H*-1-benzopyran-2-one ((*S*)-4): Application of the typical procedure with diol (*S*)-**9** (70 mg,

0.28 mmol, 1.0 equiv), collidine (74 μL, 0.56 mmol), and octanoyl chloride (58 μL, 0.34 mmol, 1.2 equiv) gave (*S*)-**4** (86 mg, 81%) as a colorless oil; $[\alpha]_D^{20} = -4.0$ ($c = 1$ in $CHCl_3$); ^{1}H NMR (300 MHz, $CDCl_3$): $\delta = 7.64$ (d, $J = 9.5$ Hz, 1H), 7.38 (d, $J = 9.2$ Hz, 1H), 6.87–6.84 (m, 2H), 6.26 (d, $J = 9.2$ Hz, 1H), 4.28–4.05 (m, 5H), 2.37 (m, 2H), 2.09–1.90 (m, 2H), 1.70–1.60 (m, 2H), 1.32–1.27 (m, 8H), 0.89 (m, 3H); ^{13}C NMR (75 MHz, $CDCl_3$): $\delta = 174.17$, 162.06, 161.29, 156.04, 143.48, 128.95, 113.42, 112.97, 112.86, 101.69, 68.52, 67.41, 65.18, 34.33, 32.79, 31.79, 29.25, 29.04, 25.09, 22.73, 14.19; HRMS(EI-MS): calcd for ($C_{21}H_{28}O_6$) $[M]^+$: 376.1886, found: 376.1887.

(*R*)-7-(3-hydroxy-4-octanoyloxybutyloxy)-2*H*-1-benzopyran-2-one ((*R*)-4): Application of the typical procedure with diol (*R*)-**9** (85 mg, 0.34 mmol, 1.0 equiv), collidine (90 μL, 0.68 mmol) and octanoyl chloride (70 μL, 0.41 mmol, 1.2 equiv) gave (*R*)-**4** (109 mg, 85%) as a colorless oil; $[\alpha]_D^{20} = +4.6$ ($c = 1$ in $CHCl_3$); HRMS(EI-MS): calcd for ($C_{21}H_{28}O_6$) $[M]^+$: 376.1886, found: 376.1885.

(*S*)-7-(3-hydroxy-4-decanoyloxybutyloxy)-2*H*-1-benzopyran-2-one ((*S*)-5): Diol (*S*)-**9** (100 mg, 0.40 mmol, 1.0 equiv) was stirred in dry pyridine (2.0 mL), and the mixture was cooled to 0°C. Decanoyl chloride (98 μL, 0.48 mmol, 1.2 equiv) was then added dropwise. After 30 min, the solution was allowed to reach room temperature and stirred overnight. The pyridine was removed in vacuo. Workup and FC as above gave (*S*)-**5** (108 mg, 67%) as a white solid. M.p. 39–41°C; $[\alpha]_D^{20} = -3.1$ ($c = 0.60$ in $CHCl_3$); ^{1}H NMR (300 MHz, $CDCl_3$): $\delta = 7.64$ (d, $J = 9.5$ Hz, 1H), 7.37 (m, 1H), 6.86–6.83 (m, 2H), 6.25 (d, $J = 9.6$ Hz, 1H), 4.27–4.10 (m, 5H), 2.36 (t, $J = 7.7$ Hz, 2H), 2.05–1.94 (m, 2H), 1.64 (m, 2H), 1.26 (br s, 12H), 0.88 (t, 6.6 Hz, 3H); ^{13}C NMR (75 MHz, $CDCl_3$): $\delta = 174.15$, 162.06, 161.29, 156.01, 143.48, 128.92, 113.37, 112.96, 112.83, 101.67, 68.49, 67.35, 65.18, 34.33, 32.78, 31.98, 29.53, 29.38 (2C), 29.27, 25.07, 22.79, 14.22; HRMS(EI-MS): calcd for ($C_{23}H_{32}O_6$) $[M]^+$: 404.2199, found: 404.2198.

(*R*)-7-(3-hydroxy-4-decanoyloxybutyloxy)-2*H*-1-benzopyran-2-one ((*R*)-5): Diol (*R*)-**9** (249 mg, 0.99 mmol, 1.0 equiv) was stirred in dry pyridine (4.0 mL), and the mixture was cooled to 0°C. Decanoyl chloride (244 μL, 1.19 mmol, 1.2 equiv) was then added dropwise. After 30 min, the solution was allowed to reach room temperature and was then stirred for other 24 h. The pyridine was removed in vacuo. Workup and FC as above gave (*R*)-**5** (276 mg, 68.6%) as a white solid. M.p. 39–41°C; $[\alpha]_D^{20} = +3.6$ ($c = 0.45$ in $CHCl_3$); HRMS(EI-MS): calcd for ($C_{23}H_{32}O_6$) $[M]^+$: 404.2199, found: 404.2200.

(*S*)-7-(3-hydroxy-4-dodecanoyloxybutyloxy)-2*H*-1-benzopyran-2-one ((*S*)-6): Application of the typical procedure with diol (*S*)-**9** (60 mg, 0.24 mmol, 1.0 equiv), collidine (64 μL, 0.48 mmol), and dodecanoyl chloride (85 μL, 0.36 mmol, 1.5 equiv) gave (*S*)-**6** (80 mg, 77%) as a white solid. M.p. 52–55°C; $[\alpha]_D^{20} = -2.2$ ($c = 0.55$ in $CHCl_3$); ^{1}H NMR (300 MHz, $CDCl_3$): $\delta = 7.64$ (d, $J = 9.6$ Hz, 1H), 7.38 (m, 1H), 6.87–6.84 (m, 2H), 6.27 (d, $J = 9.6$ Hz, 1H), 4.27–4.05 (m, 5H), 2.37 (m, 2H), 2.10–1.90 (m, 2H), 1.67–1.62 (m, 2H), 1.30–1.26 (m, 16H), 0.88 (t, 7.0 Hz, 3H); ^{13}C NMR (75 MHz, $CDCl_3$): $\delta = 174.17$, 162.04, 161.33, 155.97, 143.51, 128.92, 113.33, 112.96, 112.79, 101.62, 68.48, 67.30, 65.13, 34.31, 32.75, 32.02, 29.72 (2C), 29.58, 29.45, 29.38, 29.27, 25.06, 22.80, 14.25; HRMS(EI-MS): calcd for ($C_{25}H_{36}O_6$) $[M]^+$: 432.2512, found: 432.2510.

(*R*)-7-(3-hydroxy-4-dodecanoyloxybutyloxy)-2*H*-1-benzopyran-2-one ((*R*)-6): Application of the typical procedure with diol (*R*)-**9** (85 mg, 0.34 mmol, 1.0 equiv), collidine (90 μL, 0.68 mmol), and dodecanoyl chloride (113 μL, 0.48 mmol, 1.4 equiv) gave (*R*)-**6** (116 mg, 79%) as a white solid. M.p. 52–54°C; $[\alpha]_D^{20} = +2.1$ ($c = 0.50$ in $CHCl_3$); HRMS(EI-MS): calcd for ($C_{25}H_{36}O_6$) $[M]^+$: 432.2512, found: 432.2512.

(*S*)-7-(3-hydroxy-4-tetradecanoyloxybutyloxy)-2*H*-1-benzopyran-2-one ((*S*)-7): Application of the typical procedure with diol (*S*)-**9** (77 mg, 0.31 mmol, 1.0 equiv), collidine (82 μL, 0.62 mmol), and tetradecanoyl chloride (100 μL, 0.37 mmol, 1.2 equiv) gave (*S*)-**7** (116 mg, 81.5%) as a white solid. M.p. 62–64°C; $[\alpha]_D^{20} = -1.5$ ($c = 0.50$ in $CHCl_3$); ^{1}H NMR (300 MHz, $CDCl_3$): $\delta = 7.64$ (d, $J = 9.5$ Hz, 1H), 7.38 (m, 1H), 6.87–6.84 (m, 2H), 6.26 (d, $J = 9.5$ Hz, 1H), 4.26–4.05 (m, 5H), 2.37 (m, 2H), 2.05–1.95 (m, 2H), 1.67–1.60 (m, 2H), 1.26 (br s, 20H), 0.88 (t, $J = 6.6$ Hz, 3H); ^{13}C NMR (75 MHz, $CDCl_3$): $\delta = 174.19$, 162.04, 161.33, 156.01, 143.51, 128.94, 113.38, 112.96, 112.83, 101.65, 68.51, 67.37, 65.15, 34.33, 32.74, 32.06, 29.82, 29.78 (2C), 29.74, 29.60, 29.49, 29.40, 29.30, 25.08, 22.84, 14.27; HRMS(EI-MS): calcd for ($C_{27}H_{40}O_6$) $[M]^+$: 460.2825, found: 460.2826.

(*R*)-7-(3-hydroxy-4-tetradecanoyloxybutyloxy)-2*H*-1-benzopyran-2-one ((*R*)-7): Application of the typical procedure with diol (*R*)-**9** (70 mg, 0.28 mmol, 1.0 equiv), collidine (82 μL, 0.62 mmol), and tetradecanoyl chloride (100 μL, 0.37 mmol, 1.2 equiv) gave (*R*)-**7** (106 mg, 82.5%) as a white solid. M.p. 62–63°C; $[\alpha]_D^{20} = +1.2$ ($c = 0.50$ in $CHCl_3$); HRMS(EI-MS): calcd for ($C_{27}H_{40}O_6$) $[M]^+$: 460.2825, found: 460.2824.

(*S*)-7-(3-hydroxy-4-hexadecanoyloxybutyloxy)-2*H*-1-benzopyran-2-one ((*S*)-8): Application of the typical procedure with diol (*S*)-**9** (62 mg, 0.25 mmol, 1.0 equiv), collidine (66 μL, 0.50 mmol), and hexadecanoyl chloride (98 μL, 0.32 mmol, 1.3 equiv) gave (*S*)-**8** (91 mg, 75%) as a white solid. M.p. 70–71°C; $[\alpha]_D^{20} = -0.8$ ($c = 0.40$ in $CHCl_3$); ^{1}H NMR (300 MHz, $CDCl_3$): $\delta = 7.64$ (d, $J = 9.6$ Hz, 1H), 7.38 (m, 1H), 6.87–6.83 (m, 2H), 6.26 (d, $J = 9.6$ Hz, 1H), 4.29–4.05 (m, 5H), 2.36 (m, 2H), 2.08–1.90 (m, 2H), 1.64 (m, 2H), 1.26 (br s, 24H), 0.88 (m, 3H); ^{13}C NMR (100 MHz, $CDCl_3$): $\delta = 174.18$, 162.04, 161.32, 155.99, 143.50, 128.92, 113.35, 112.95, 112.81, 101.63, 68.49, 67.33, 65.14, 34.31, 32.75, 32.05, 29.82, 29.81 (2C), 29.77 (2C), 29.73, 29.59, 29.49, 29.38, 29.28, 25.07, 22.82, 14.26; HRMS(EI-MS): calcd for ($C_{29}H_{44}O_6$) $[M]^+$: 488.3138, found: 488.3139.

(*R*)-7-(3-hydroxy-4-hexadecanoyloxybutyloxy)-2*H*-1-benzopyran-2-one ((*R*)-8): Application of the typical procedure with diol (*R*)-**9** (77.5 mg, 0.31 mmol, 1.0 equiv), collidine (85μL, 0.62 mmol), and hexadecanoyl chloride (140 μL, 0.47 mmol, 1.5 equiv) gave (*R*)-**8** (118 mg, 78.2%) as a white solid. M.p. 69–70°C; $[\alpha]_D^{20} = +0.7$ ($c = 0.45$ in $CHCl_3$); HRMS(EI-MS): calcd for ($C_{29}H_{44}O_6$) $[M]^+$: 488.3138, found: 488.3140.

Enzyme assays: All substrates were diluted from stock solutions in DMSO and stored at −20°C. All buffers were prepared with MilliQ deionized water. BSA (2 mg mL^{-1}) and $NaIO_4$ (1 mM) was prepared in advance in aqueous borate (20 mM) at pH 8.8. Enzymes were diluted from 1 mg mL^{-1} stock solutions of the supplied solid in borate buffer. Assays (0.1 mL) were followed in individual wells of round-bottom polypropylene 96-well-plates (Costar) by using a Cytofluor II Fluorescence Plate Reader (PerSeptive Biosystems, filters $\lambda_{ex} = 360 \pm 20$, $\lambda_{em} = 460 \pm 20$ nm). Fluorescence data were converted to umbelliferone concentration by means of a calibration curve.

Acknowledgements

This work was supported by the Swiss National Science Foundation, the Office Fédéral Suisse de L'Education et de la Science, the COST Action D16, and Protéus SA, Nîmes, France. We thank Prof. Thomas Ward, Prof. Hans-Beat Bürgi and Dr. Jürg Hauser for helpful discussions in statistical analysis, and Dr. Jean-Philippe Goddard for assistance in data processing.

Keywords: activity profiles · cluster analysis · enzymes · fingerprints · fluorescent probes

[1] a) B. Marrs, S. Delagrave, D. Murphy, *Curr. Opin. Microbiol.* **1999**, *2*, 241 – 245; b) W. P. C. Stemmer, *Proc. Natl. Acad. Sci. USA* **1994**, *91*, 10747 – 10751; c) W. P. C. Stemmer, *Nature* **1994**, *370*, 389 – 391; d) L. You, F. H. Arnold, *Protein Eng.* **1996**, *9*, 77 – 83; e) M. T. Reetz, K.-E. Jaeger, *Chem. Eur. J.* **2000**, *6*, 407 – 412; f) S. V. Taylor, P. Kast, D. Hilvert, *Angew. Chem.* **2001**, *113*, 3408 – 3436; *Angew. Chem. Int. Ed.* **2001**, *40*, 3310 – 3335.

[2] For a recent review see: J.-L. Reymond, D. Wahler, *ChemBioChem* **2002**, *3*, 701 – 708.

[3] a) *Enzyme Assays: A Practical Approach* (Eds.: R. Eisenthal, M. Danson), Oxford University Press, **2002**; b) S. Gul, S. K. Sreedharan, K. Brocklehurst, *Enzyme Assays: Essential Data*, Wiley, **1998**.; c) M. T. Reetz, *Angew. Chem.* **2001**, *113*, 292 – 320; *Angew. Chem. Int. Ed.* **2001**, *40*, 284 – 310; d) D. Wahler, J.-L. Reymond, *Curr. Opin. Chem. Biol.* **2001**, *5*, 152 – 158; e) F. Beisson, A. Tiss, C. Rivière, R. Verger, *Eur. J. Lipid Sci. Technol.* **2000**, 133 – 153; f) D. Wahler, J.-L. Reymond, *Curr. Opin. Biotechnol.* **2001**, *12*, 535 – 544.

[4] a) F. Badalassi, D. Wahler, G. Klein, P. Crotti, J.-L. Reymond, *Angew. Chem.* **2000**, *112*, 4233 – 4236; *Angew. Chem. Int. Ed.* **2000**, *39*, 4067 – 4070; b) D. Wahler, F. Badalassi, P. Crotti, J.-L. Reymond, *Angew. Chem.* **2001**, *113*, 4589 – 4592; *Angew. Chem. Int. Ed.* **2001**, *40*, 4457 – 4460; c) D. Wahler, F. Badalassi, P. Crotti, J.-L. Reymond, *Chem. Eur. J.* **2002**, *8*, 3211 – 3228; d) J.-L. Reymond, D. Wahler, F. Badalasssi, H. K. Nguyen, WO0192563, **2001**.

[5] a) E. M. González-Garciá, J. Grognux, D. Wahler, J.-L. Reymond, *Helv. Chim. Acta* **2003**, *86*, 2458 – 2470; b) E. Nyfeler, J. Grognux, D. Wahler, J.-L. Reymond, *Helv. Chim. Acta* **2003**, *86*, 2919 – 2927.

[6] We chose green-purple instead of red-green to code enantioselectivity because this contrast is better perceived by color-blind people.

[7] http://www.unesco.org/idams; http://www.visualstats.org

[8] *Introduction to Multivariate Analysis* (Eds.: C. Chatfield, A. J. Collins), Chapman and Hall, London, **1983**.

Received: September 26, 2003
Revised: January 15, 2004

